

SUPPLEMENTARY INFORMATION

**Synthesis of urea from CO<sub>2</sub> and N<sub>2</sub> fixation  
under mild conditions using polarized  
hydroxyapatite as catalyst**

**Jordi Sans,<sup>a</sup> Marc Arnau,<sup>a</sup> Ricard Bosque,<sup>a</sup> Pau Turon<sup>b,\*</sup> and  
Carlos Alemán<sup>a,c,\*</sup>**

*<sup>a</sup> Departament d'Enginyeria Química and Barcelona Research Center in Multiscale  
Science and Engineering, Universitat Politècnica de Catalunya, EEBE, C/ Eduard  
Maristany 10-14, 08019, Spain*

*<sup>b</sup> B. Braun Surgical, S.A.U., Carretera de Terrassa 121, 08191 Rubí (Barcelona), Spain*

*<sup>c</sup> Institute for Bioengineering of Catalonia (IBEC), The Barcelona Institute of Science  
and Technology, Baldori Reixac 10-12, 08028 Barcelona Spain*

*E-mail: [pau.turon@bbraun.com](mailto:pau.turon@bbraun.com) and [carlos.aleman@upc.edu](mailto:carlos.aleman@upc.edu)*

## **METHODS**

### **Synthesis of Hydroxyapatite (HAp)**

15 mL of 0.5 M  $(\text{NH}_4)_2\text{HPO}_4$  in de-ionized water were added at a rate of 2 mL/min to 25 mL of a 0.5 M of  $\text{Ca}(\text{NO}_3)_2$  solution in ethanol with pH previously adjusted to 11 using ammonium hydroxide solution. The mixture was left aging for 1 h under gentle agitation (150 rpm) at room temperature. Hydrothermal treatment at 150 °C was applied using an autoclave Digestec DAB-2 for 24 h. The autoclave was allowed to cool down before opening. The precipitates were separated by centrifugation and washed with water and a 60/40 v/v mixture of ethanol/water (twice). After lyophilizing it for 3 days, a white powder was obtained. The HAp powder was extensively grinded to reduce aggregates and homogenize the grain size, this step being crucial for the nanostructure of the HAp scaffold (see below).

### **Synthesis of Pluronic® F-127 hydrogel**

25 g of distilled water was mixed with 25 g of Pluronic® F-127 polymer using a FlackTek SpeedMixer at 3500 rpm for 5 minutes. After that, 50 g of Pluronic® polymer were added and vigorously stirred using the same conditions. The resultant hydrogel was stored at 4 °C.

### **Preparation of nanoporous HAp scaffolds**

HAp powder was extensively grinded to reduce aggregates and homogenize the grain size, this step being crucial for the nanostructure of the HAp scaffold. Then, 60% wt. of previously prepared Pluronic® F-127 hydrogel was slowly added to the grinded HAp powder in a cold room at 4 °C. In order to achieve a homogeneous mixture, such addition process was periodically interrupted for stirring at 2500 rpm for a 2 min minutes using a

Fisherbrand™ Digital Vortex Mixer. The obtained white paste was left aging at 4 °C for 24 h to ensure the homogeneous distribution of the hydrogel. The resulting ink was modeled using a cold spatula (< 4 °C) to obtain 3D HAp scaffolds with the desired shape. The utilization of the cold spatula allowed to reduce the friction between the metal and the paste without compromising the homogeneity of the shaped samples. Finally, the scaffolds were calcined at 1000 °C using a muffle Carbolite ELF11/6B/301 for 2 h. In this step, the Pluronic® F-127 hydrogel was completely removed from the modeled scaffold.

### **Thermal polarization for the catalytic activation of nanoporous HAp**

Calcined HAp scaffolds were catalytically activated by placing the samples between two stainless steel plates (AISI 304), which acted as electrodes. The HAp sample was left in control with negative electrode, while the positive electrode was separated 4 cm from the calcined scaffold. A constant DC voltage of 500 V was applied for 1 h with a GAMMA power supply, while the temperature was kept at 1000 °C. Samples were allowed to cool down maintaining the applied electric potential for 30 minutes, and finally, all the system was powered off and left to cool down overnight.

### **Characterization**

Morphological characterization was performed by scanning electron microscopy (SEM) using a Focused Ion Beam Zeiss Neon40 microscope equipped with a SEM GEMINI column with a Shottky field emission. Samples were sputter-coated with a thin layer of carbon to prevent sample charging problems.

High-resolution transmission electron experiments were carried out in a JEOL JEM J2100 microscope, equipped with a LaB6 thermionic electron gun and operated at an accelerating voltage of 200 keV. Images were recorded using a Gatan Orius CCD camera.

Raman analyses were performed by means of an inVia Qontor confocal Raman microscope (Renishaw) equipped with a Renishaw Centrus 2957T2 detector and a 532 nm laser. In order to obtain representative data, 32 single point spectra were averaged.

Electrochemical impedance spectroscopy (EIS) studies were performed using a Multi Autolab/M101 from Metrohm connected to a conductivity meter cell by means of two stainless steel electrodes AISI 304 isolated by a resin holder. Measurements were performed in the 100 kHz – 10 mHz frequency range and applying a 100 mV sinusoidal voltage. Approximately 50  $\mu$ L of a 3.5 % saline solution was dispensed on p-HAp and HAp samples to enhance the conductivity and minimize noise. Then, soaked samples were placed between the two electrodes and EIS measurements were performed. Electrical Equivalent Circuits (EECs) were obtained by fitting the experimental data.

### **Synthesis of urea**

The reactor consisted in an inert reaction chamber coated with a perfluorinated polymer (120 mL), in which both the catalyst and water (20 mL) were incorporated. The reactor was equipped with an inlet valve for the entrance of N<sub>2</sub> and CO<sub>2</sub> and an outlet valve to recover the gaseous reaction products. A UV lamp (GPH265T5L/4, 253.7 nm) was also placed in the middle of the reactor to irradiate the catalyst directly, the lamp being protected by a UV transparent quartz tube. All surfaces were coated with a thin film of a perfluorinated polymer in order to avoid any contact between the reaction medium and the reactor surfaces, in this way discarding other catalyst effects.

Reactions were performed at temperatures ranging from 60 to 120 °C for a reaction time comprised between 6 and 48 h. Both the p-HAp catalyst and 20 mL of de-ionized liquid water were initially incorporated into the reaction chamber (reactions were performed separately for each catalyst). A vacuum pump was used in order to eliminate the initial air content of the reaction chamber. Each selected gas was introduced to increase the reaction chamber pressure (measured at room temperature) to the target pressure. The chamber pressure was increased up to a pressure comprised between 1 and 6 bar by introducing sequentially each feeding reaction gas (half and half).

### **Reaction with engine exhaust gases**

Engine exhaust gases were collected from the exhaust pipe of a gasoline passenger car manufactured in 2007 (Mazda 3) by means of a MSHA portable pump and stored into a Tedlar® gas sampling bag (LB-2 Septa). According to the European Regulation EURO4, the CO<sub>2</sub> : NO<sub>x</sub> ratio in the emissions of such vehicle is 1962.5. The extraction of gases from the exhaust pipe was carried out by revolutionizing the engine of the car at approximately 3500 rpm. After incorporating the catalyst and 20 mL of de-ionized liquid water in the reactor described above, the collected engine exhaust gas was introduced into the reaction chamber (1 bar). The reaction was conducted at 120 °C for 24 h. The reaction products were analyzed by <sup>1</sup>H NMR spectroscopy, following the procedures described for the urea reactions.

### **Analyses of the reaction products**

The reaction products were analyzed by <sup>1</sup>H NMR spectroscopy. All <sup>1</sup>H NMR spectra were acquired with a Bruker Avance-II+ spectrometer operating at 600 MHz. The chemical shift was calibrated using tetramethylsilane (TMS) internal standard. 512 scans

were recorded in all cases. In order to remove the reaction products from the catalyst, 10 mg of the reacted catalyst were dissolved in 15 mL of water with pH adjusted to  $2.1 \pm 0.2$  using 7.6 mM  $\text{H}_2\text{SO}_4$ , to promote the conversion of ammonia in  $\text{NH}_4^+$ , and applying 4 cycles that involved sonication (5 min) and stirring (1 min) steps. Then, for the  $^1\text{H}$  NMR sample preparation, 500  $\mu\text{L}$  of the reacted catalyst solution were mixed with 100  $\mu\text{L}$  of  $\text{DMSO-}d_6$  instead of solvents with labile deuterons (*i.e.*  $\text{D}_2\text{O}$ ) to avoid the formation of ammonium deuterated analogues, not desired for quantitative analysis. The same treatment was applied to the water supernatant.

Initially,  $^1\text{H}$  NMR spectra were acquired using the watergate suppression method, which was reported to be very useful to identify products coming from  $\text{N}_2$  fixation, as for example  $\text{NH}_4^+$ . Unfortunately, the urea signal almost overlapped water signal and, therefore, the application of the strong water signal suppression (zgcppr pulse sequence) was necessary to quantify urea. However, the zgcppr was too aggressive for the rest of products, which were lost. Therefore, spectra were recorded in duplicate using both the watergate and the zgcppr methods.

As mentioned in the main text, further analysis of the reactions products was performed using a Micro-Chromatograph AGILENT 3000 ( $\mu\text{PGC}3000$ ) through the storage of the reactions gas products in Tedlar® sampling bags (Screw Cap Valve, 1 Liter, 30272-U).

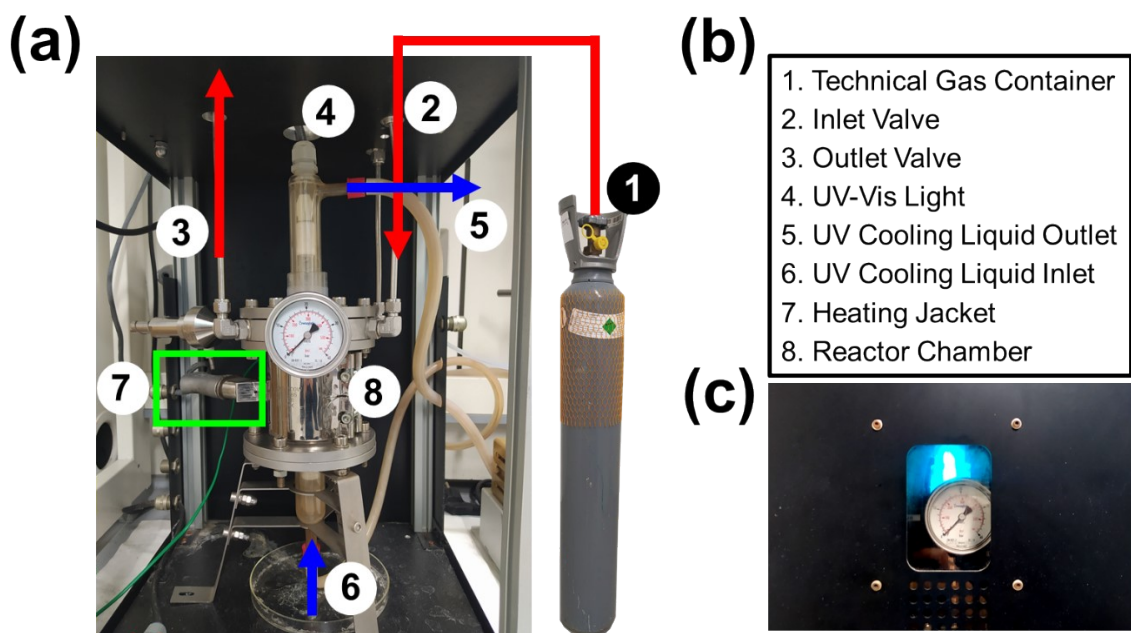


**Figure S1.** (a): Catalysis batch reactor set-up used for the experimental reactions. (b): Legend of the elements appearing in Image (a). (c): Protective cover for UV-Vis light experiments.

## RESULTS AND DISCUSSION

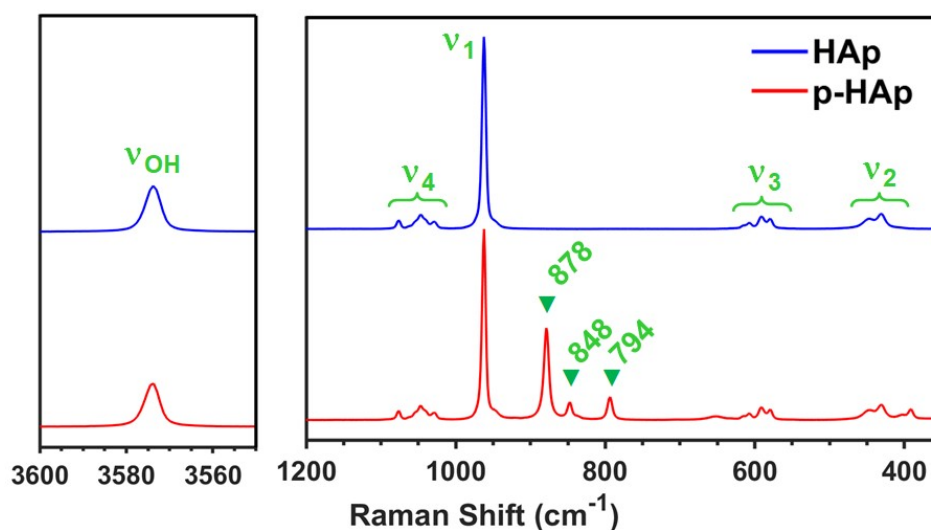


**Figure S2.** (a) Raman spectra and Nyquist plot of calcined HAp and polarized HAp (p-HAp). The Raman spectrum of HAp is dominated by the  $\text{PO}_4^{3-}$  characteristic vibrations at  $\nu_1=962\text{ cm}^{-1}$  (symmetric stretching mode of the P–O bonds),  $\nu_2=400\text{-}490\text{ cm}^{-1}$  (doubly degenerated O–P–O bending mode),  $\nu_3=570\text{-}625\text{ cm}^{-1}$  (triply degenerated asymmetric P–O stretching mode) and  $\nu_4=1020\text{-}1095\text{ cm}^{-1}$  (triply degenerated O–P–O bending model), and the  $\text{OH}^-$  characteristic stretching vibration at  $\nu_{\text{OH}}=3574\text{ cm}^{-1}$ .<sup>25,26</sup> After catalytic activation by applying the calcination and the electro-thermal polarization steps, the resulting p-HAp samples exhibited enhanced crystallinity ( $\chi_c$ ) and generation of  $\text{OH}^-$  vacancies. The increment of crystallinity, which was quantified by examining the full width at half maximum (FWHM) of the  $\nu_1$  peak  $\nu_1$  7.2 and 6.4  $\text{cm}^{-1}$  for HAp and p-HAp, respectively), was of 19.2% ( $\chi_c=0.78 \pm 0.02$  and  $0.93 \pm 0.02$  for HAp and p-HAp, respectively). Besides, the generated  $\text{OH}^-$  vacancies were quantified by evaluating the  $\nu_{\text{OH}} : \nu_1$  ratio, which decreased from 0.26 for HAp to 0.17 for p-HAp. The Raman spectrum of p-HAp reflects the apparition of three peaks at 878, 848, and 794  $\text{cm}^{-1}$ , which correspond to the  $\text{HPO}_4^{2-}$  normal vibration mode, and the POH deformation and rotation modes characteristic of brushite ( $\text{CaHPO}_4 \cdot 2\text{H}_2\text{O}$ ), respectively.<sup>25,26</sup> The apparition of such calcium phosphate phase at the surface of the catalyst was achieved by separating 4 cm the positive electrode from the calcined HAp sample, which was kept in contact with the negative electrode, during the application of the external DC electric field (step 4 of process used to prepare p-HAp). Previous studies showed that the incorporation of brushite phase at the surface of p-HAp creates synergistic effects that increases the efficiency and selectivity of HAp-based catalysts.<sup>25,26</sup>



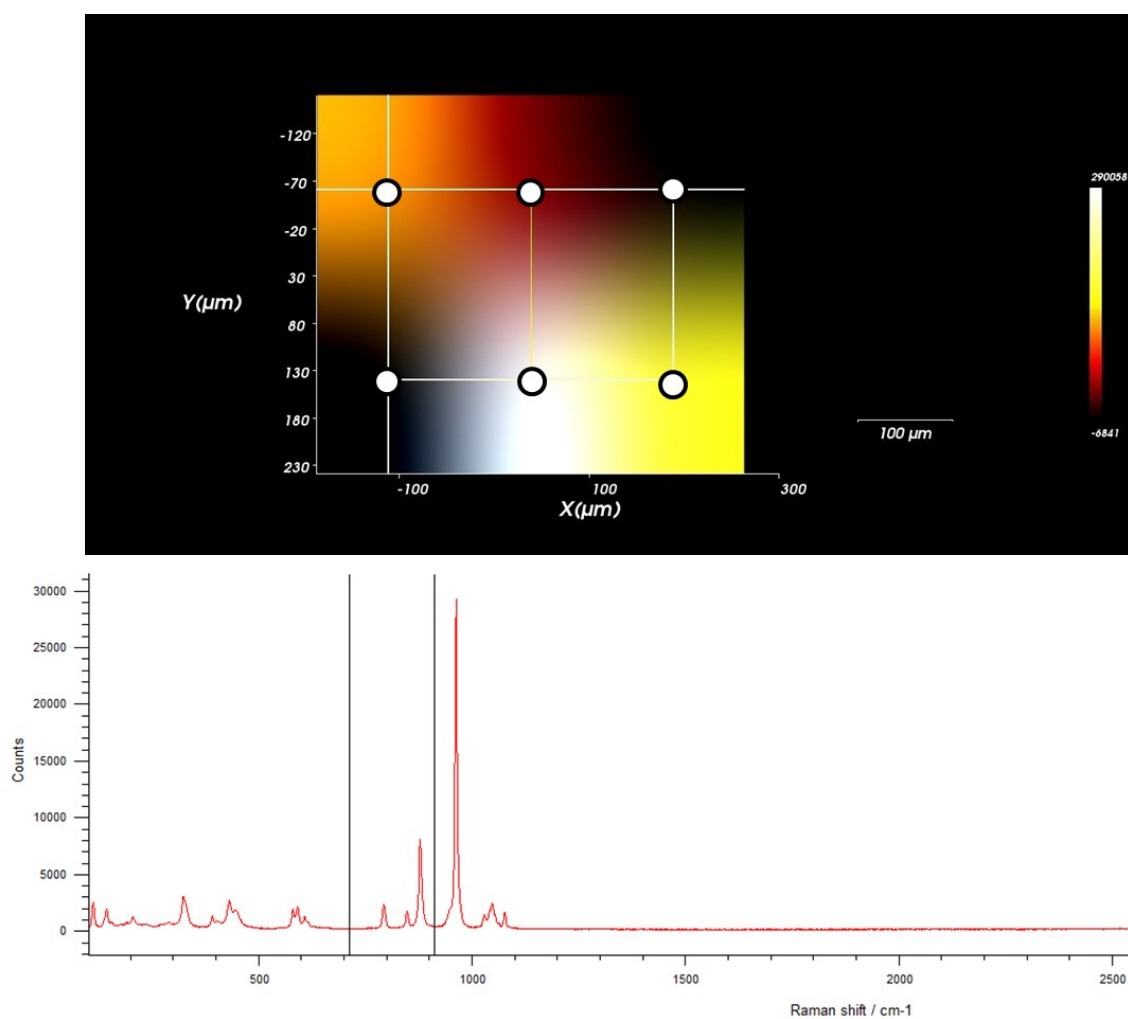


**Figure S3.** Representative map depicting the distribution of brushite on the surface of p-HAp by means of acquiring Raman spectra corresponding to a 2×3 grid. The map was generated considering the signal to baseline of the brushite characteristic region (as seen in the figure).

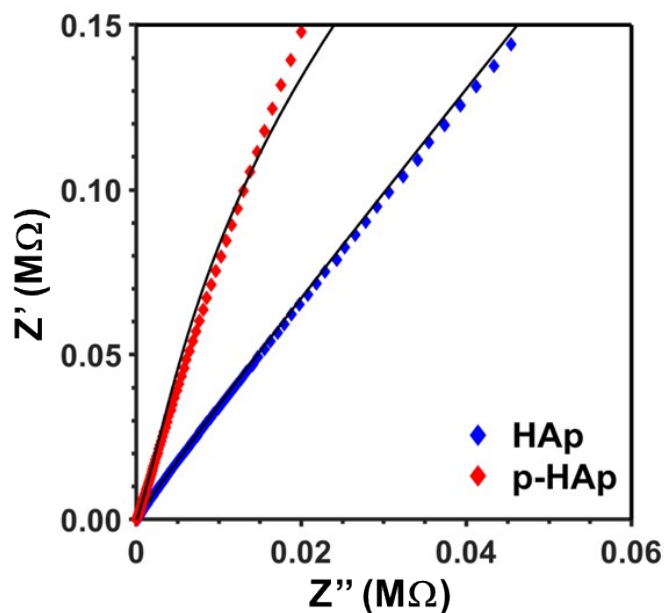


**Figure S4.** Nyquist plots obtained from EIS measurements on p-HAp and HAp. EIS measurements were conducted on wetted p-HAp and HAp samples, which were placed between two stainless steel electrodes isolated by a resin holder.<sup>28</sup> The obtained Nyquist plots are fully consistent with those reported for catalytically active and inactive HAp, respectively, evidencing the success of the thermal polarization. Although both p-HAp and HAp exhibited capacitive spikes due to the fast charge transport expected for wetted samples, the one obtained for p-HAp approached more to the imaginary axis, reflecting a much higher capacitive behaviour. Moreover, the resistance obtained by adjusting the derived data to an already reported equivalent electrical circuit<sup>29</sup> (Figure S4) was lower for p-HAp than for HAp ( $R_b = 1.6$  and  $9.7 \text{ M}\Omega/\text{cm}^2$ ).

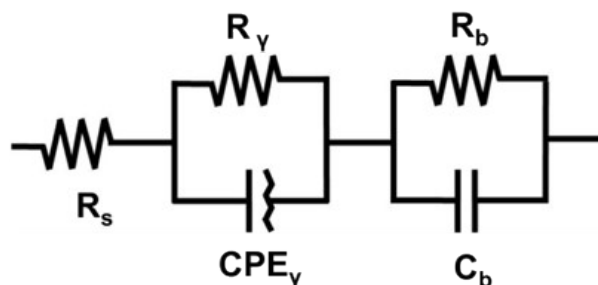


**Figure S5.** Electric Equivalent Circuit (EEC) developed to explain the electrical and capacitive properties of catalytically active p-HAp.

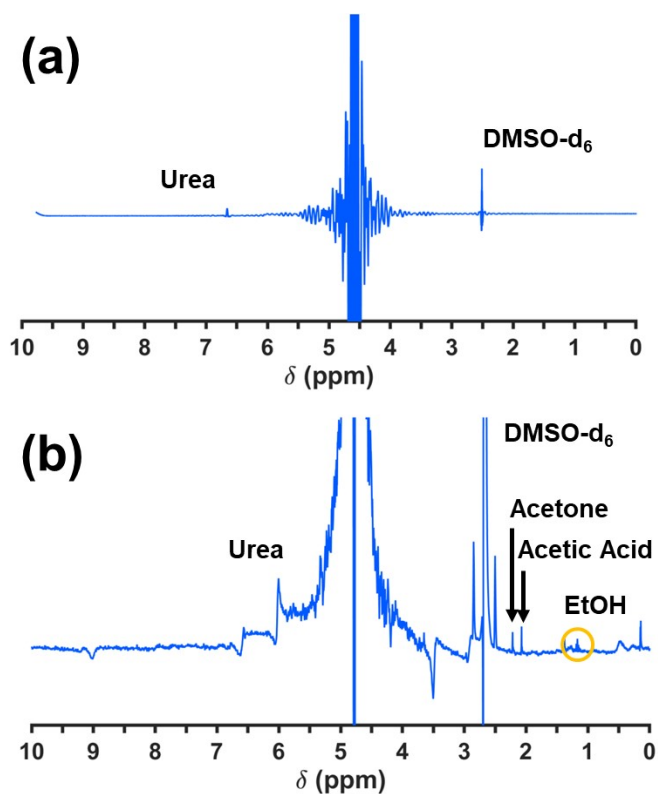


**Figure S6.** Representative  $^1\text{H}$  NMR spectra used to identify the reaction products in the dissolved catalyst: (a) spectrum with suppressed water signal (zgcppr pulse sequence); and (b) spectrum with attenuated water signal (watergate). The reaction was conducted with UV illumination at 120 °C for 48 h using a mixture of 3 bar of  $\text{CO}_2$  and 3 bar of  $\text{N}_2$ , 20 mL of de-ionized water and nanoporous p-HAp as catalyst.

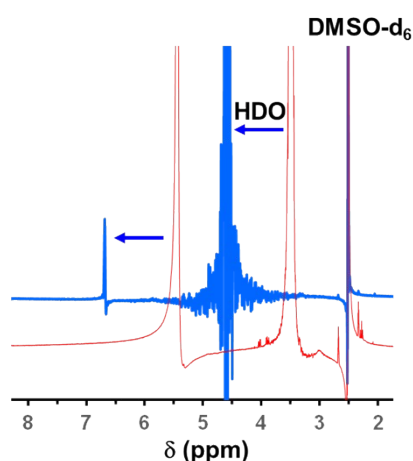


**Figure S7.** Comparison of the spectrum used to identify the reaction products in the supernatant (acid pH) recorded using suppressed water signal (thick blue line) with the spectrum obtained for a calibration aqueous solution with urea and  $\text{DMSO-}d_6$  (neutral pH) (thin red line). The pH-induced shift of the peaks associated to urea and HDO is shown. The peak of  $\text{DMSO-}d_6$  is not affected by the pH.

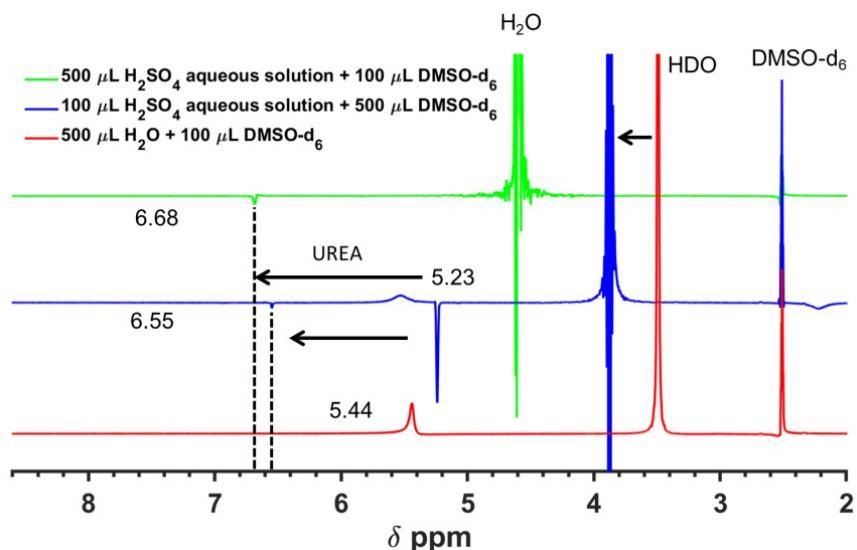


**Figure S8.** Study on the shift of the urea peak with the acidity of the solution. The acidity has been controlled by increasing the amount of  $\text{H}_2\text{SO}_4$

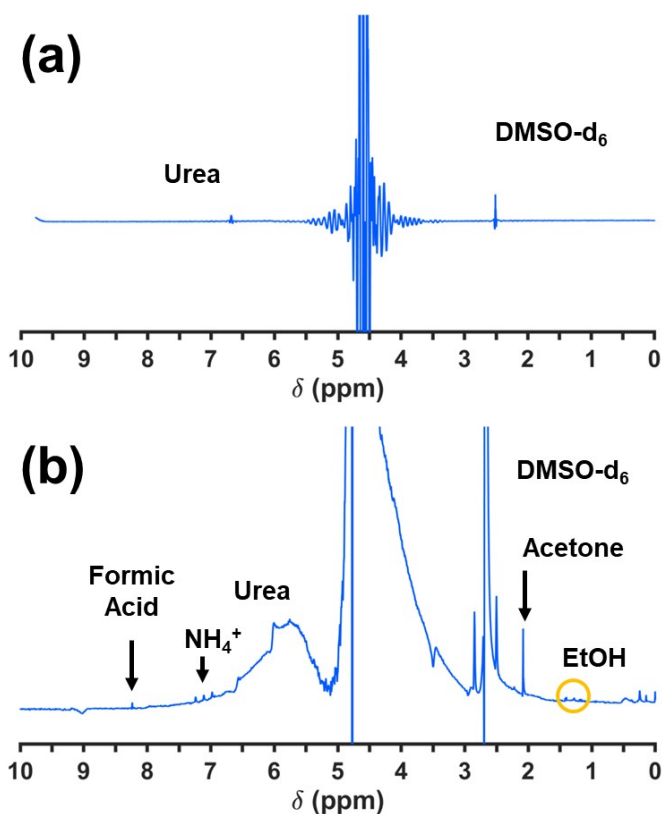


**Figure S9.** Representative  $^1\text{H}$  NMR spectra used to identify the reaction products in the supernatant: (a) spectrum with suppressed water signal (zgcppr pulse sequence); and (b) spectrum with attenuated water signal (watergate). The reaction was conducted with UV illumination at 120  $^\circ\text{C}$  for 48 h using a mixture of 3 bar of  $\text{CO}_2$  and 3 bar of  $\text{N}_2$  /  $\text{NO}$  (314 ppm of  $\text{NO}$ ), 20 mL of de-ionized water and p-HAp as catalyst.

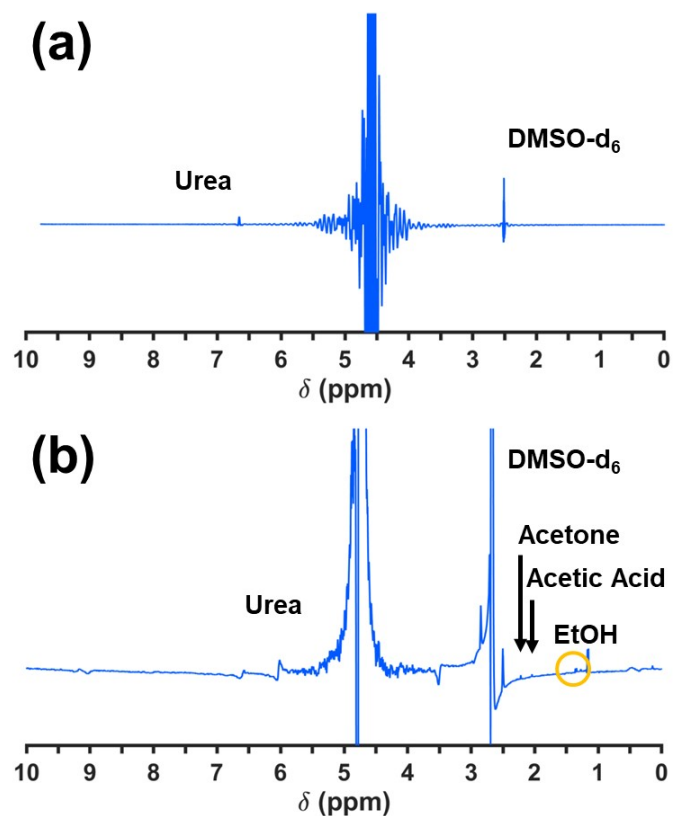


**Figure S10.** Representative  $^1\text{H}$  NMR spectra used to identify the reaction products in the dissolved catalyst: (a) spectrum with suppressed water signal (zgcppr pulse sequence); and (b) spectrum with attenuated water signal (watergate). The reaction was conducted with UV illumination at 120 °C for 48 h using a mixture of 3 bar of  $\text{CO}_2$  and 3 bar of  $\text{N}_2$  / NO (314 ppm of NO), 20 mL of de-ionized water and p-HAp as catalyst.

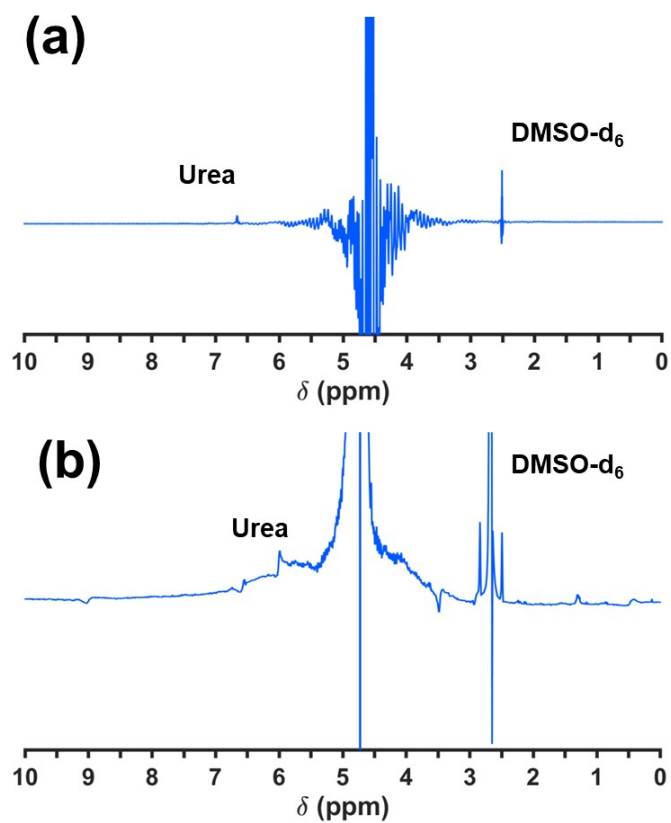


**Figure S11.** Representative <sup>1</sup>H NMR spectra used to identify the reaction products in the supernatant: (a) spectrum with suppressed water signal (zgcppr pulse sequence); and (b) spectrum with attenuated water signal (watergate). The reaction was conducted without UV illumination at 120 °C for 48 h using a mixture of 3 bar of CO<sub>2</sub> and 3 bar of N<sub>2</sub> / NO (314 ppm of NO), 20 mL of de-ionized water and p-HAp as catalyst.

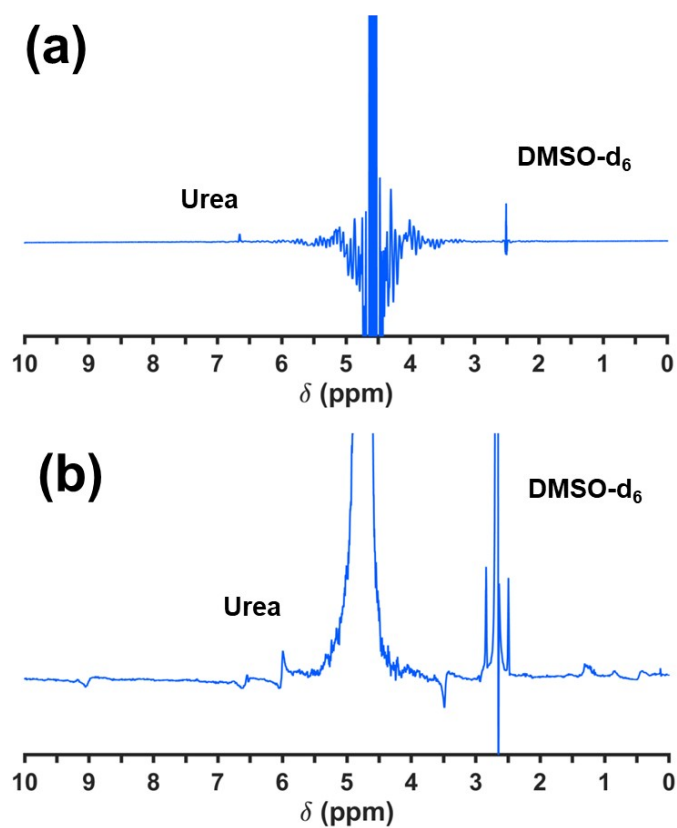


**Figure S12.** Representative <sup>1</sup>H NMR spectra used to identify the reaction products in the dissolved catalyst: (a) spectrum with suppressed water signal (zgcppr pulse sequence); and (b) spectrum with attenuated water signal (watergate). The reaction was conducted without UV illumination at 120 °C for 48 h using a mixture of 3 bar of CO<sub>2</sub> and 3 bar of N<sub>2</sub> / NO (314 ppm of NO), 20 mL of de-ionized water and p-HAp as catalyst.

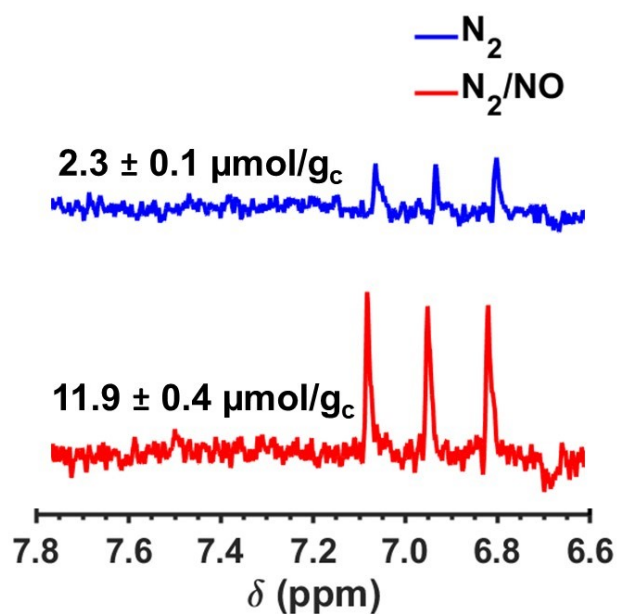


**Figure S13.** <sup>1</sup>H-NMR spectra of the NH<sub>4</sub><sup>+</sup> product region for reactions conducted without UV illumination at 120 °C for 24 h, 20 mL of de-ionized water and p-HAp as catalyst with the following gas mixtures: 1) in red, N<sub>2</sub> / NO (314 ppm of NO) and 2) in blue, sole N<sub>2</sub>. The yields are normalized by catalyst weight and can be observed at the right part of the triplet.



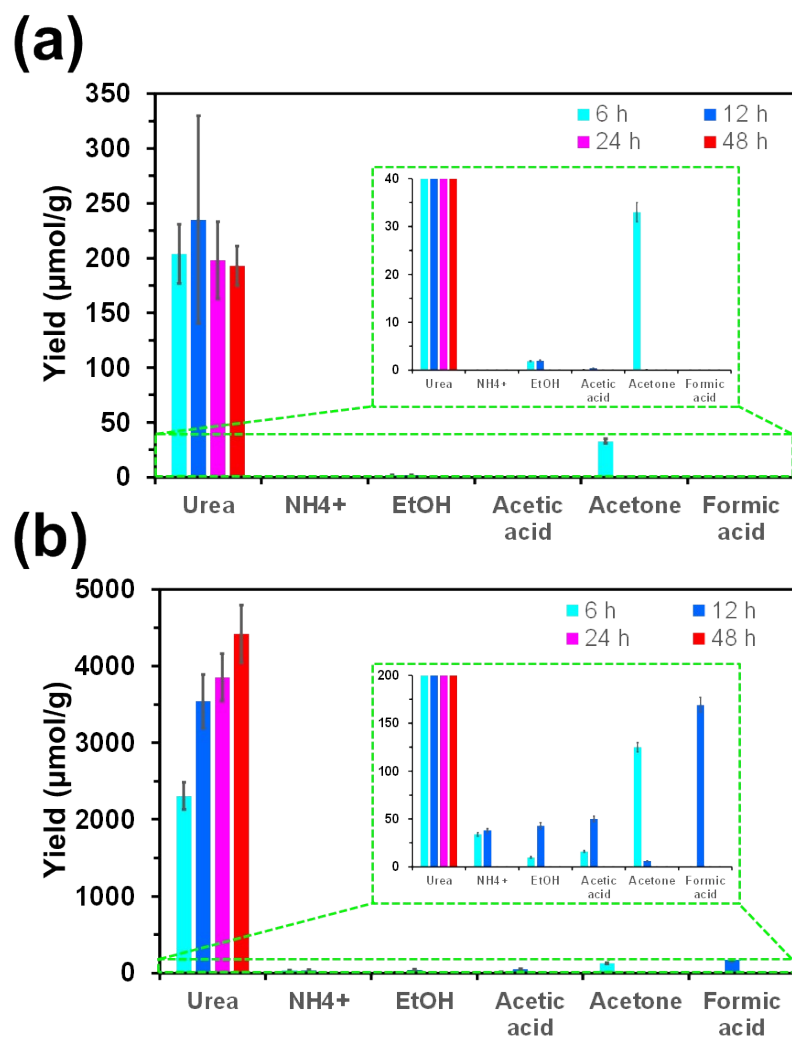


**Figure S14.** Yield of the reaction products identified by  $^1\text{H}$  NMR in (a) the catalyst and (b) the supernatant at different reaction times (6, 12, 24 and 48 h) for a mixture of 3 bar of  $\text{CO}_2$  and 3 bar of  $\text{N}_2$  / NO (314 ppm of NO). In all cases the reaction was conducted without UV illumination at 120 °C using 20 mL of de-ionized water and p-HAp as catalyst.

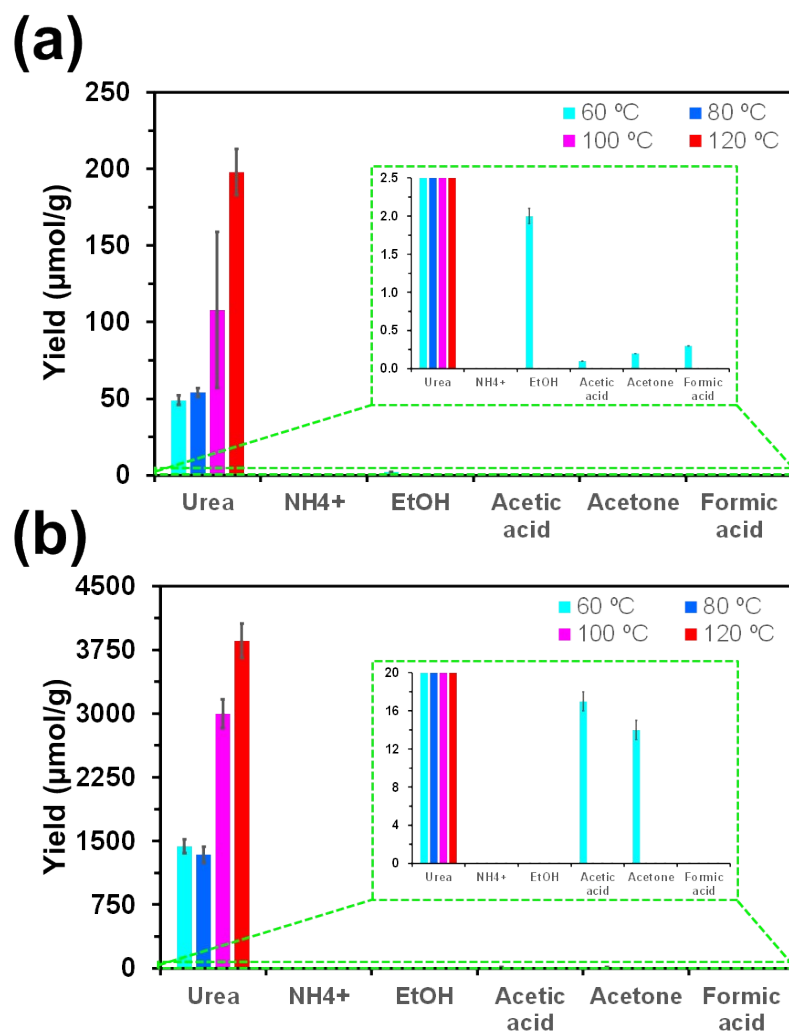


**Figure S15.** Yield of the reaction products identified by  $^1\text{H}$  NMR in (a) the catalyst and (b) the supernatant for reactions conducted at different temperatures (60, 80, 100, 120 °C) for a mixture of 3 bar of  $\text{CO}_2$  and 3 bar of  $\text{N}_2$  / NO (314 ppm of NO). In all cases the reaction was conducted without UV illumination for 24h using 20 mL of de-ionized water and p-HAp as catalyst.

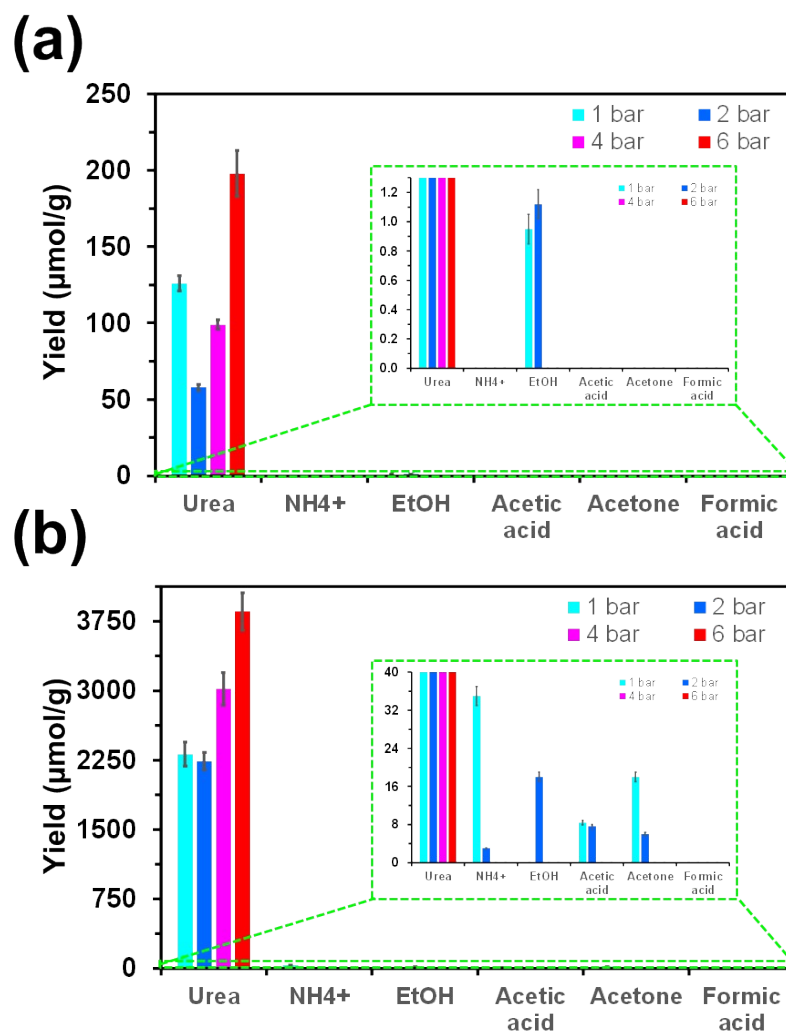


**Figure S16.** Yield of the reaction products identified by  $^1\text{H}$  NMR in (a) the catalyst and (b) the supernatant for reactions conducted at different pressures (1, 2, 4 and 6 bar; half and half of  $\text{CO}_2$  and  $\text{N}_2$  /  $\text{NO}$  with 314 ppm of  $\text{NO}$  in the latter). In all cases the reaction was conducted without UV illumination for 24h at 120 °C using 20 mL of de-ionized water and p-HAp as catalyst.

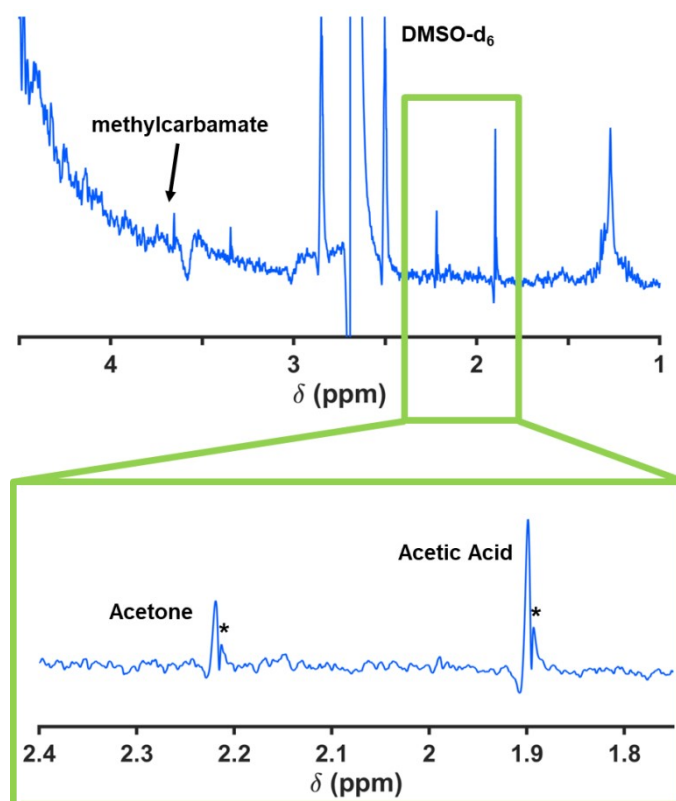


**Figure S17.** Representative  $^1\text{H}$  NMR spectrum used to identify the presence of carbamate ions in the supernatant. The reaction was conducted without UV illumination at  $120\text{ }^\circ\text{C}$  for 24 h using 6 bar of  $\text{CO}_2$ , 19 mL of liquid  $\text{H}_2\text{O}$  and 1 mL of  $\text{NH}_3$ . The spectrum was obtained in non-acidic conditions and using the watergate acquisition method.

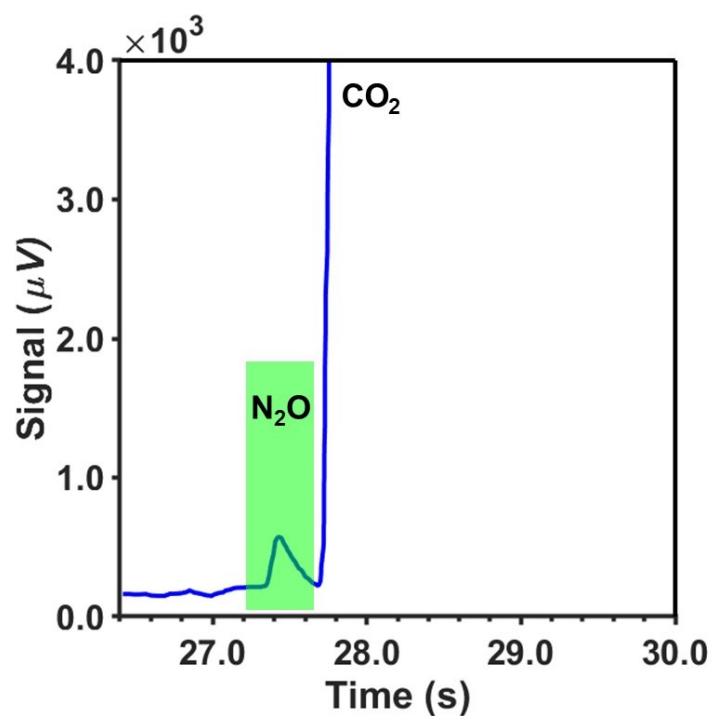


**Figure S18.** Micro-gas chromatography detected signal versus retention time where the small peak detected for the  $N_2O$  can be appreciated almost overlapping with the  $CO_2$  one. No computational quantification was possible due to low presence of the product; however, its assignment is certain since the equipment was previously calibrated with a pure  $N_2O$  standard to ensure precise determination of its retention time.

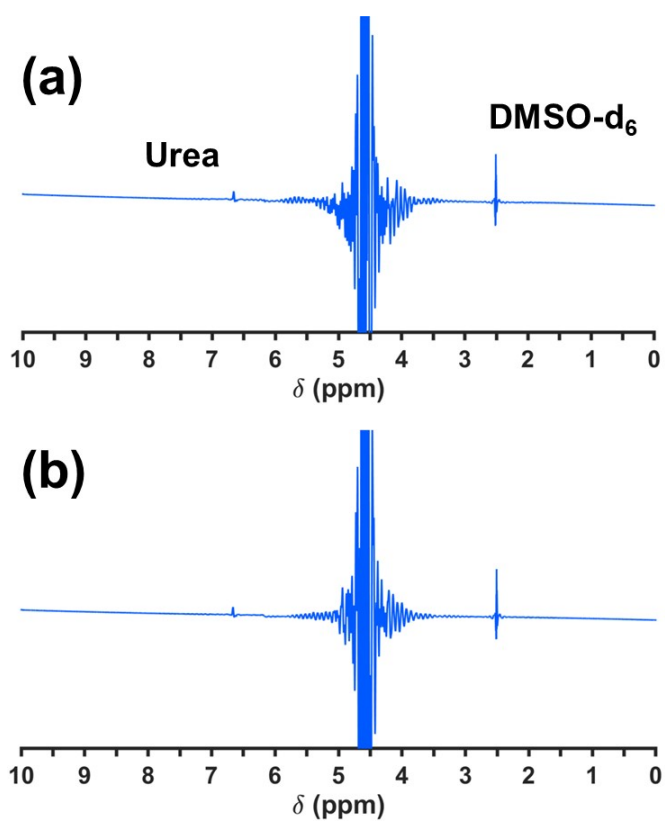


**Figure S19.** Representative  $^1\text{H}$  NMR spectra used to identify the yield of urea in (a) the dissolved catalyst and (b) the supernatant. The reaction was conducted without UV illumination at 120 °C for 24 h using 1 bar of fumes from gasoline vehicle engines, 20 mL of de-ionized water and p-HAp as catalyst.